MedChemComm

CONCISE ARTICLE

The structure–activity relationships of L3MBTL3 inhibitors: flexibility of the dimer interface†

Michelle A. Camerino,[a] Nan Zhong,[b] Aiping Dong,[b] Bradley M. Dickson,[a] Lindsey I. James,[a] Brandi M. Baughman,[a] Jacqueline L. Norris,[a] Dmitri B. Kireev,[a] William P. Janzen,[a] Cheryl H. Arrowsmith[abcd] and Stephen V. Frye*[a]

We recently reported the discovery of UNC1215, a potent and selective chemical probe for the L3MBTL3 methyllysine reader domain. In this article, we describe the development of structure–activity relationships (SAR) of a second series of potent L3MBTL3 antagonists which evolved from the structure of the chemical probe UNC1215. These compounds are selective for L3MBTL3 against a panel of methyllysine reader proteins, particularly the related MBT family proteins, L3MBTL1 and MBTD1. A co-crystal structure of L3MBTL3 and one of the most potent compounds suggests that the L3MBTL3 dimer rotates about the dimer interface to accommodate ligand binding.

Introduction

Histone post translational modifications such as lysine methylation play an important role in the function of chromatin by creating binding sites for reader proteins. This binding event leads to downstream signalling *via* the recruitment and stabilization of chromatic template machinery and is an essential step in the regulation of chromatin and gene expression.[1,2] Histone lysine methylation can signal either the activation[3,4] or repression[5–7] of gene transcription, depending on the site and degree of methylation.[8] Lysine methylation has been identified in various positions of the histone tails, mainly on histone 3 at positions H3K4 (lysine 4), H3K9, H3K27, H3K36, H3K79 and on histone four at position H4K20.[9] The ε-amino group of a lysine at any of these positions can be mono (me1), di (me2) or tri-methylated (me3), thus changing the chemical properties of this residue from a small, relatively "hard" positive charge to a more diffuse, "soft" and polarizable positive charge in the case of Kme3.[10] In most cases, the binding site of this methylated residue is a hydrophobic 'aromatic cage', a conserved structural motif in almost all reader proteins.[11] In our previous studies, we have focussed on the recognition of lysine methylation by MBT domain methyllysine readers, a subclass in the 'Royal family' of proteins that includes the proteins L3MBTL1, L3MBTL3, and MBTD1 among others.[12,13] While these proteins have been associated with haematopoiesis[14] and cancer biology,[15,16] their exact biological mechanisms still require elucidation. For this reason, we have endeavoured to identify small molecule chemical probes that would facilitate further study and understanding of these proteins.[17] To date, we have reported the discovery of weak small molecule inhibitors of L3MBTL1 such as UNC669,[18,19] and have most recently identified a potent and selective chemical probe, UNC1215, for the L3MBTL3 methyllysine reader domain (Fig. 1).[20] Interestingly, the high potency and selectivity of UNC1215 can be explained by its co-crystal structure with L3MBTL3 which shows that UNC1215 binds as a 2 : 2 dimer with the protein.[20] This was the first published evidence of L3MBTL3 dimerization and has prompted further studies in our group. Here we report a second series of L3MBTL3 inhibitors, their structure–activity relationships and their potential unique interactions with the L3MBTL3 dimer.

aCenter for Integrative Chemical Biology and Drug Discovery, Division of Chemical Biology and Medicinal Chemistry, University of North Carolina Eshelman School of Pharmacy, University of North Carolina at Chapel Hill, Chapel Hill, North Carolina, USA. E-mail: svfrye@email.unc.edu; Fax: +1 919 843 8465; Tel: +1 919 843-5486

bStructural Genomics Consortium, University of Toronto, Ontario, Canada

cDepartment of Medical Biophysics, University of Toronto Ontario, Canada

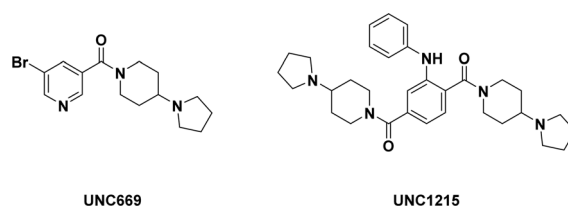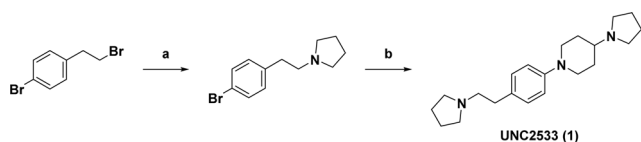*dPrincess Margaret Cancer Centre, 101 College Street, Toronto, Ontario, Canada, M5G 1L7*

Fig. 1 Previously reported inhibitors of L3MBTL1 (UNC669) and L3MBTL3, (UNC1215).

Results and discussion

In our efforts to develop additional, novel inhibitors of the methyllysine reader, L3MBTL1, we simulated putative apo-homodimer conformations of L3MBTL1 and L3MBTL3 using a recently developed scheme for free energy computations.[21] In each case, we observed stable homodimers with more compact ligand pockets than those observed in the UNC1215–L3MBTL3 co-crystal structure.[20] Based on this observation, new small molecules were proposed as possible ligands that could fit within the more compact homodimer pockets while preserving the dibasic character of UNC1215, which we knew was required for potent dimer binding. Following Scheme 1, we synthesised the dibasic compound UNC2533 (1) and identified it as a potent inhibitor of the L3MBTL3 methyllysine reader domain. *In vitro* evaluation of UNC2533 in an AlphaScreen® methylated histone peptide competition assay[22] yielded an IC_{50} of 62 ± 7.2 nM for L3MBTL3 which is within three-fold of the chemical probe UNC1215 ($IC_{50} = 24 ± 7.6$ nM, Table 1).[20]‡ The activity of UNC2533 was confirmed by isothermal titration calorimetry (ITC), to give a K_d of 0.37 μM which is also within 3-fold of the reported dissociation constant of UNC1215 ($K_d = 0.12$ μM).[20] Biological screening of UNC2533 against the other readers in our panel (Table 1) showed a similar selectivity profile to UNC1215. UNC2533 binds L3MBTL1 weakly ($IC_{50} = 14 ± 0.0$ μM) with a similar affinity to the L3MBTL1 inhibitor UNC669[18,19] ($IC_{50} = 21 ± 1.2$ μM). The weak binding affinity for L3MBTL1 was also confirmed by ITC ($K_d = 19.0$ μM), showing that UNC2533 is 50 times more selective for L3MBTL3 over L3MBTL1. As the L3MBTL1 monomer is known to bind UNC669 *via* key interactions between the pyrrolidine and the aromatic reader pocket in domain 2,[18] it is reasonable to suggest that one or both of the pyrrolidines in UNC2533 is responsible for its weak L3MBTL1 activity. UNC2533 also displays modest activity against the other royal family protein MBTD1, as well as 53BP1, a member of the Tudor domain family. Other readers from the chromodomain family (CBX7), the Tudor domain family (UHRF1), and the PHD finger family of zinc-binding proteins (PHF23 and Jarid1A) did not bind to UNC2533 ($IC_{50} > 30$ μM).

The X-ray co-crystal structure of UNC2533 and L3MBTL3

To investigate the potential binding mode of UNC2533 to L3MBTL3, the X-ray co-crystal structure of the complex was determined and refined to 2.3 Å (PDB ID: 4L59). Despite being a smaller molecule than UNC1215, UNC2533 also binds L3MBTL3 as a 2 : 2 complex. Each molecule of UNC2533 bridges the L3MBTL3 dimer interface by interacting with domain 1 of one monomer and the presumed histone methyllysine binding site in domain 2 of the other monomer (Fig. 2a). The binding interaction to domain 2 is primarily mediated by a strong hydrogen bond (2.6 Å) between the carboxylate oxygen of D381 and the pyrrolidine nitrogen of the (pyrrolidinyl)piperidine moiety (Fig. 2b). Additional hydrophobic contacts and a cation–π interaction between the positively charged pyrrolidine nitrogen and the domain 2 aromatic cage strengthen binding. The interaction of UNC2533 with domain 1 is mediated by a second hydrogen bond (2.8 Å) between the carboxylate oxygen of D274 and the C2-linked pyrrolidine nitrogen. Further hydrophobic contacts between the pyrrolidine ring and Y301 reinforce binding in this pocket. Atomic distances for the key binding interactions in the UNC1215–L3MBTL3 complex[20] and the UNC2533–L3MBTL3 complex were measured using MOE software.[23] All key contacts between the ligand and the protein were very similar in distance and strength (ESI Table 5†). This result was surprising as UNC2533 is significantly smaller in size than UNC1215. The intramolecular distance between the two basic nitrogens in UNC2533 is 10.4 Å. The equivalent intramolecular distance for the UNC1215 molecule is 13.1 Å. This difference indicates that a change in the conformation of the L3MBTL3 dimer must have occurred to maintain its bonding interactions with the smaller inhibitor, UNC2533.

To compare the UNC1215–L3MBTL3 complex with the UNC2533–L3MBTL3 complex we aligned selected backbone chains with Kabsch's method[24] as implemented in the molecular dynamics program VMD.[25] Visualization of the entire 2 : 2 complex shows that the dimer interface has rotated slightly such that only one of the two monomers in the UNC2533–L3MBTL3 complex is aligned with the UNC1215–L3MBTL3 complex (Fig. 3). For the "aligned" monomers, there is very little structural variation in the domain 1 and domain 2 binding pockets. Upon closer inspection of the domain 2 (methyllysine) binding pocket we found that all of the key residues are closely aligned with the exception of some flexibility in the side chains (Fig. 4a). Similarly, the conformation of the domain 1 binding pocket is also well conserved, with the exception of the E410 side chain which has flipped its orientation due to a steric clash with the phenyl ring of UNC1215 (Fig. 4b). In contrast, all of the key residues in the "misaligned" monomers have shifted. Measurement of the distances between the alpha carbons of residue pairs in the binding site of each crystal structure shows a shift of between 2.4 and 4.6 Å (Fig. 4c and d, ESI Table 6†). The same results were observed when the alternate monomer was aligned using Kabsch's method.[24] These findings reveal that the L3MBTL3 dimer primarily accommodates binding of the smaller UNC2533 molecule by rotating the two L3MBTL3 monomers at the dimer interface rather than altering the

Scheme 1 Synthetic route to UNC2533 (1). *Reagents and conditions*: (a) pyrrolidine, K_2CO_3, CH_3CN, room temperature, 16 h, 58% yield (b) 4-(pyrrolidin-1-yl)piperidine, XPhos, $Pd_2(dba)_3$, Cs_2CO_3, dioxane/water, microwave irradiation, 110 °C for 20 min, then 125 °C for 3 h, 12% yield.

‡ It should be noted that the Alphascreen® activities of UNC1215, UNC669 and UNC1079 are slightly different in various publications due to changes in the assay format – readers should refer to the supplemental information for the exact conditions that were used for the assays in this publication.

Table 1 The activity of UNC2533 (**1**) compared to control compounds determined from AlphaScreen® and ITC. Compounds screened against L3MBTL1 and MBTD1 were screened at concentrations of up to 300 μM in the AlphaScreen®. All other proteins were screened with a maximal compound concentration of 30 μM

#	Structure	Activity as determined by AlphaScreen® IC$_{50}$ (μM) and ITC K_d (μM), shows in parentheses [ ]							
		L3MBTL3	L3MBTL1	MBTD1	53BP1	CBX7	UHRF1	Jarid1A	PHF23
UNC2533 (**1**)		0.062 ± 0.0072 [0.37 ± 0.052]	14 ± 0.0 [19 ± 1.4]	53 ± 4	14.5 ± 2.1	>30	>30	>30	>30
UNC669		2.8 ± 0.57	21 ± 1.2	>300	>30	>30	>30	>30	>30
UNC1079		8.0 ± 3.0	170 ± 31	50 ± 8.8	>30	>30	>30	>30	>30
UNC1215		0.024 ± 0.0076 [0.12 ± 0.11]^a	8.9 ± 0.40 [9.4 ± 1.7]^a	78 ± 2.5	13.7 ± 2.0	>30	>30	>30	>30

^{a} Indicates literature values.
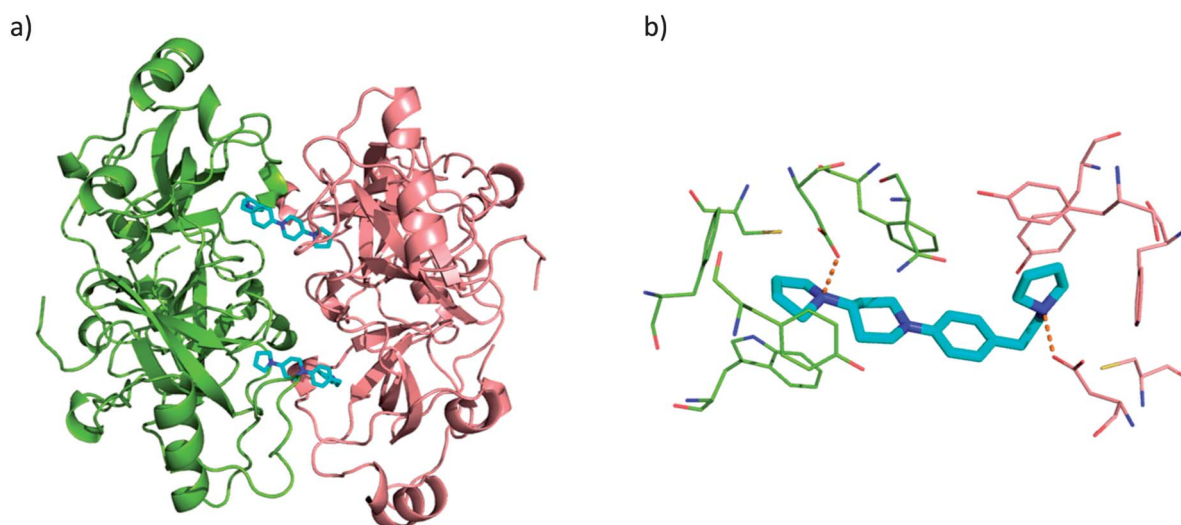
Fig. 2 (a) X-ray crystal structure of UNC2533 (**1**) in complex with L3MBTL3 as a 2 : 2 complex (PDB ID: 4L59). UNC2533 is shown in cyan and the two monomers of L3MBTL3 are colored in green and pink. (b) The binding site of UNC2533 with L3MBTL3 at the dimer interface showing the key hydrogen bonding interactions of the ligand with residues D381 and D274.

conformation of the protein backbone in the ligand binding site. This flexibility at the dimer interface could be a mechanism that endogenous L3MBTL3 uses to read different histone sequences. Whether this mechanism is truly important to the biological function of L3MBTL3 is the subject of ongoing studies.

Structure–activity relationships

As the central core of the UNC2533 molecule is structurally distinct from UNC1215, we further investigated how changes in this structure would affect its activity and selectivity for L3MBTL3. We first synthesised a series of compounds that

explored modifications to the (pyrrolidinyl)piperidine, the pyrrolidine, and the C2-linker. Synthesis was performed following the methods exemplified in Schemes 1 or 2 and as described in the ESI.† Briefly, compounds were synthesised from the commercially available 1-bromo-4-(2-bromoethyl)benzene *via* an alkylation reaction followed by cross coupling (Scheme 1). For Buchwald couplings, the reaction conditions were improved by employing a RuPhos/RuPhos pre-catalyst system, with NaO*t*-Bu as the base and tetrahydrofuran as the solvent.[26] These conditions were more suitable for the coupling of cyclic amines affording the desired products in superior yields (18–98%) within a shorter reaction time. Under microwave irradiation, complete conversion to the product was often observed by
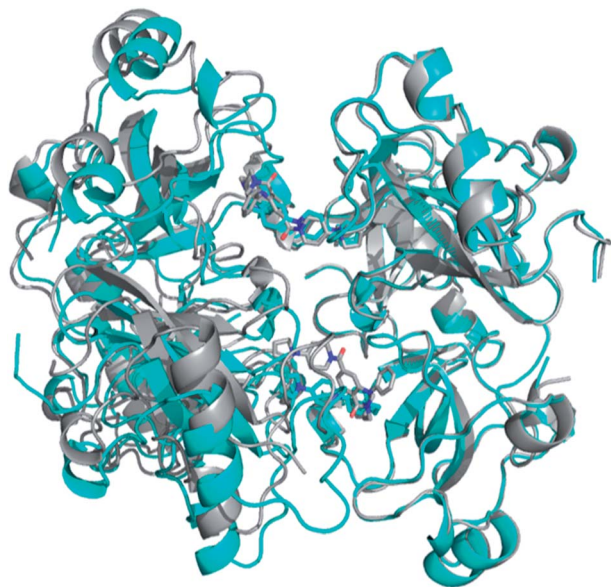
Fig. 3 Alignment of the UNC2533–L3MBTL3 crystal structure (PDB ID: 4L59, cyan) with the UNC1215–L3MBTL3 crystal structure (PDB ID: 4FL6, grey) using the Kabasch method implemented in VMD. The monomer on the right is aligned while the one on the left is misaligned.
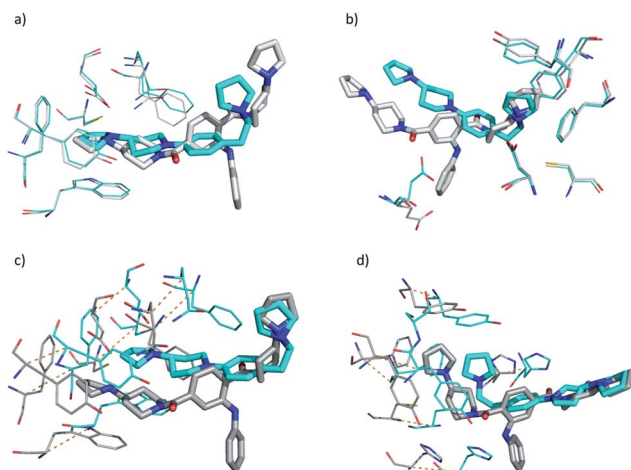

Fig. 4 Superimposition of the UNC1215–L3MBTL3 complex (PDB ID: 4FL6, grey carbons) and the UNC2533–L3MBTL3 complex (PDB ID: 4L59, cyan carbons) (a) view of the domain 2 (methyllysine) binding pocket showing residues in the aligned monomer (b) view of the domain 1 binding pocket showing residues in the aligned monomer (c) view of the domain 2 (methyllysine) binding pocket showing the shifted residues in the misaligned monomer (d) view of the domain 1 (methyllysine) binding pocket showing the shifted residues in the misaligned monomer.

LCMS after 10 minutes of heating. If the di-bromo starting material was unavailable, compounds were synthesised from the acid *via* an initial amide coupling. A Buchwald coupling followed by reduction of the amide with LiAlH$_4$ gave the final dibasic compounds (Scheme 2.).

The biological activity of all compounds was primarily evaluated against our reader panel using the AlphaScreen® assay.[22] Previously reported compounds UNC1215 [20] and UNC669 [18,19]
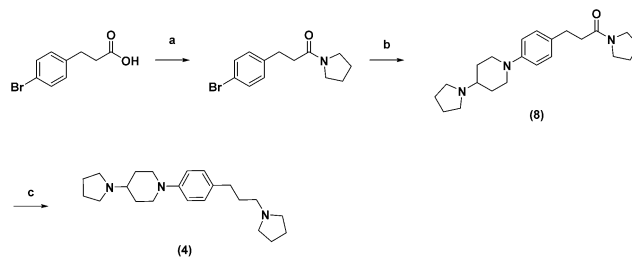
Scheme 2 *Reagents and conditions*: (a) pyrrolidine, TBTU, NEt$_3$, DMF, room temperature, 17 h (b) 4-(pyrrolidin-1-yl)piperidine, RuPhos, RuPhos pre-catalyst, NaO*t*-Bu, THF, microwave irradiation, 120 °C, 10 min (c) LiAlH$_4$, THF, reflux, 18 h.
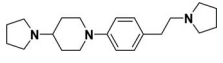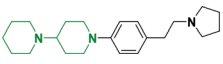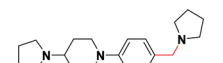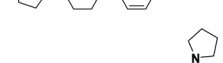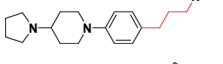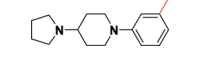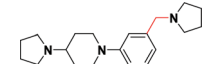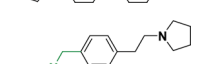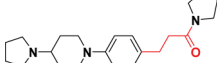
were used as positive controls for L3MBTL3 and L3MBTL1, respectively. UNC1079 [20] was used as a less active control as it binds L3MBTL3 poorly (IC$_{50}$ = 8.0 ± 3.0 μM). As we were most interested in the selectivity of the compounds for L3MBTL3 against the other MBT family proteins L3MBTL1 and MBTD1, compounds evaluated at these proteins were tested at concentrations of up to 300 μM. All other assays were carried out with a maximal compound concentration of 30 μM. While Alpha-Screen® is a suitable method for the high-throughput screening of compounds, an orthogonal assay, such as isothermal titration calorimetry (ITC) was used to confirm SAR for a representative subset of compounds.

We initially modified the (pyrrolidinyl)piperidine moiety to a slightly larger 1,4′-bipiperidine in compound **2** (Table 2). As desired, the L3MBTL1 activity of this compound decreased to 50 ± 3.2 μM. Unfortunately this small change also resulted in a 9-fold drop in activity for L3MBTL3 which was mirrored in the ITC by a 7-fold loss in activity (K_d = 2.4 μM). This indicates that binding to the L3MBTL3 dimer is primarily mediated by the interaction of the (pyrrolidinyl)piperidine with the second methyllysine reader domain.

Next, we set out to synthesise compounds of different sizes by modifying the length and position of the 2-carbon linker. Shortening the linker to a single methylene, in compound **3** resulted in a 4 to 5-fold drop in L3MBTL3 activity (IC$_{50}$ = 0.35 ± 0.11 μM, K_d = 1.4 μM), which could be due to a weaker interaction of this compound with either or both of the domain 1 and domain 2 binding sites of the L3MBTL3 dimer. Lengthening the linker to a 3-carbon chain in compound **4** maintained L3MBTL3 activity in the Alphascreen® and is consistent with the ability of a larger molecule like UNC1215 to be accommodated in the binding site. Compound **4**, however, was less active against L3MBTL3 by ITC, which gave a K_d of 1.84 μM. Moving the 2-carbon chain *meta* to the piperidine in (compound **5**) did not result in a significantly different IC$_{50}$ (0.12 ± 0.023 μM) however the ITC showed much weaker binding (K_d = 2.7 μM) indicating that substitution at this position is not well tolerated. The shorter methylene linker in the *meta* position (**6**) had similar activity to **5**.

Confident that the piperidine moiety acts simply as a linker group in both UNC2533 and UNC1215, we modified the piperidine to a 2-carbon aliphatic chain in compound **7**. This change resulted in a 20-fold loss in potency against L3MBTL3 such that its activity was similar to the monobasic compound

Concise Article

Table 2 Effects of changing the (pyrrolidinyl)piperidine or the ethyl-pyrrolidine
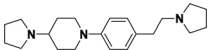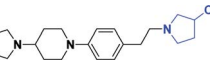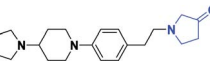
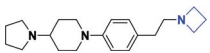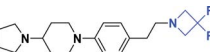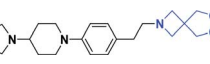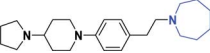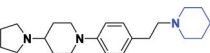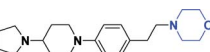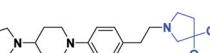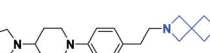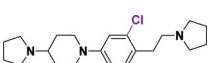| #	Structure	Activity as determined by AlphaScreen® IC$_{50}$ (µM) and ITC K_d (µM), shows in parentheses [ ]							
		L3MBTL3	L3MBTL1	MBTD1	53BP1	CBX7	UHRF1	Jarid1A	PHF23
UNC2533 (**1**)		0.062 ± 0.0072 [0.37 ± 0.052]	14 ± 0.0 [19 ± 1.4]	53 ± 4	14.5 ± 2.1	>30	>30	>30	>30
2		0.58 ± 0.027 [2.4 ± 0.13]	50 ± 3.2	170 ± 39	>30	>30	>30	>30	>30
3		0.35 ± 0.11 [1.4 ± 0.13]	57 ± 0.17	157 ± 38	>30	>30	>30	>30	>30
4		0.070 ± 0.013 [1.8 ± 0.38]	10 ± 2.8	135 ± 33	>30	>30	>30	>30	>30
5		0.12 ± 0.051 [2.7 ± 0.33]	30 ± 2.6	261 ± 34	>30	>30	>30	>30	>30
6		0.12 ± 0.023	45 ± 4.9	78 ± 17	19.4 ± 2.9	>30	>30	>30	>30
7		1.3 ± 0.87	51 ± 4.0	94 ± 11	>30	>30	>30	>30	>30
8		2.4 ± 1.0 [38 ± 2.2]	>300	>300	>30	>30	>30	>30	>30
9		2.4 ± 0.28	88 ± 10	>300	>30	>30	>30	>30	>30
10		0.32 ± 0.11	32 ± 2.1	149 ± 8.5	>30	>30	>30	>30	>30
11		13 ± 1.4 [44 ± 4.9]	90 ± 1.1 [48, $n = 1$]	58 ± 1.9	>30	>30	>30	>30	>30

UNC669, and is potentially due to the inability of this smaller compound to engage both pockets of the dimer. To determine if two basic amines are critical to maintaining L3MBTL3 activity, we synthesised the corresponding amide, compound **8**, and found that this modification decreased L3MBTL3 activity by more than 30-fold. This loss in activity was also evident by ITC, where only weak binding was observed (K_d = 38 µM). The same trend was observed when comparing compounds **6** and **9** and is rationalised by the crystal structure of UNC2533, which shows that a strong ionic interaction occurs between the positively charged nitrogen of the ethyl-pyrrolidine and the carboxylate of D274 in domain 1. To decrease linker flexibility, the 2-carbon chain was replaced with the more rigid piperidine in symmetrical compound **10**. As a result, the L3MBTL3 affinity was weakened about 5-fold (0.32 ± 0.11 µM). This loss in activity could be explained by the UNC2533 crystal structure which shows that it is necessary for the ethylene linker to adopt a gauche conformation in-order to engage the carboxylate of D274. A flatter geometry may not be able to achieve this

efficiently. As expected, complete removal of the ethyl pyrrolidine in compound **11**, resulted in over a 200 fold loss in L3MBTL3 activity (IC$_{50}$ = 13 ± 1.4 µM), indicating that while this fragment still binds, both amines are required for high L3MBTL3 potency. In comparison with UNC2533, the activity of **11** at L3MBTL1 was lower (IC$_{50}$ = 90 ± 1.1 µM), indicating that the ethyl pyrrolidine is somewhat responsible for the observed L3MBTL1 binding of UNC2533.

With the knowledge that a two carbon linker is optimal for activity, we continued by modifying the aromatic core and the ethyl-pyrrolidine of UNC2533 (Table 3). Addition of a chloro *ortho* to the 2-carbon linker in compound **22** was tolerated, however no significant increase in potency was observed. Hypothesizing that we may be able to increase compound selectivity by designing a covalent inhibitor, we synthesised the electrophilic 3-cyano and 3-keto compounds **12** and **13** that could be susceptible to nucleophilic attack by the cysteine thiol present in the domain 1 or domain 2 binding pockets. Both compounds were evaluated in the same AlphaScreen® assay. After an incubation time of 30

MedChemComm

Table 3 Effects of substituting the pyrrolidine moiety and core aromatic

#	Structure	Activity as determined by AlphaScreen® IC$_{50}$ (µM) and ITC K_d (µM), shows in parentheses [ ]							
		L3MBTL3	L3MBTL1	MBTD1	53BP1	CBX7	UHRF1	Jarid1A	PHF23
UNC2533 (**1**)		0.062 ± 0.0072	14 ± 0.0	53 ± 4	14.5 ± 2.1	>30	>30	>30	>30
12		0.36 ± 0.039	128 ± 15	>300	>30	>30	>30	>30	>30
13		0.39 ± 0.24	44 ± 5.5	166 ± 34	18.4 ± 6.5	>30	>30	>30	>30
14		0.048 ± 0.013	86 ± 12	>300	>30	>30	>30	>30	>30
15		1.0 ± 0.55	152 ± 28	>300	>30	>30	>30	>30	>30
16		0.059 ± 0.035 [0.40 ± 0.17]	60 ± 9.9 [30, $n = 1$]	>300	>30	>30	>30	>30	>30
17		0.10 ± 0.038	63 ± 2.1	249 ± 2.8	>30	>30	>30	>30	>30
18		0.080 ± 0.041 [0.61 ± 0.13]	50 ± 5.5 [3.3 ± 0.15]	290 ± 9.2	>30	>30	>30	>30	>30
19		0.85 ± 0.091	125 ± 14	>300	>30	>30	>30	>30	>30
20		0.65 ± 0.095	92 ± 14	>300	>30	>30	>30	>30	>30
21		0.27 ± 0.005	65 ± 9.9	247 ± 17	>30	>30	>30	>30	>30
22		0.037 ± 0.0017	21 ± 9.7	176 ± 71	21.0 ± 3.5	>30	>30	>30	>30

minutes, both modifications displayed a 5-fold drop in potency (Table 3), suggesting that covalent inhibition of L3MBTL3 seems unlikely and that substitution at the 3-position of the pyrrolidine ring is sub-optimal for ligand binding. As no significant improvement over UNC2533 was observed, these compounds were not pursued further.

Further modifications to the ethyl-pyrrolidine by increasing the size of the pyrrolidine ring to either an azepane (**17**) or piperidine (**18**) did not significantly change the L3MBTL3 activity. The L3MBTL3 activity of **18** was confirmed by ITC yielding a K_d of 0.61 µM for L3MBTL3. Surprisingly, the K_d of **18** for L3MBTL1 was more potent than expected based on the Alphascreen® results ($K_d = 3.3$ µM) and is currently under further investigation. Introduction of a hydrogen bond acceptor to the six-membered ring was originally hypothesised to have favourable interactions with the tyrosine hydroxyl located at the back of the domain 1 binding pocket however the inclusion of oxygen in the morpholino compound **19** was not tolerated. The activity for this compound was weakened by more than an order of magnitude when compared to the alicyclic compound. This may be due to the decreased basicity of the morpholino nitrogen compared with the pyrrolidine nitrogen. From the crystal structure of UNC2533, it is also reasonable to suggest that this may be the result of an unfavourable electronic clash between the electronegative oxygen atom and the pi electrons of

the nearby Y301. A loss in activity was also observed for the spirocyclic compounds **20** and **21** which may undergo similar electronic clashes with the binding site.

Decreasing the ring size to an azetidine gave the equipotent compound **14** (*versus* UNC2533). Interestingly, this compound was also more selective than UNC1215 against L3MBTL1 and MBTD1 in our Alphascreen® assay. Further modification to this moiety by introduction of a difluoro in the 3-position of the azetidine ring in **15** dropped the L3MBTL3 activity to 1 µM. Calculation of the pK_a of the azetidine nitrogen in both compounds revealed that addition of the difluoro decreases the pK_a from 10.3 to 7.1 and consequently weakens the ionic interaction of the pyrrolidine N with D274. The hydrolysed spirocyclic, compound **16** had a similar activity and selectivity profile to the unsubstituted azetidine (**14**) suggesting that the hydroxyl groups are not making new favourable interactions but are also not interfering with binding. ITC of **16** confirmed the activity of this compound for L3MBTL3, yielding a K_d of 0.40 µM. The selectivity against L3MBTL1 was also confirmed by ITC to be 75 fold ($K_d = 30$ µM).

Conclusions

In summary, we have reported the discovery of a second series of L3MBTL3 inhibitors based on our original compound

UNC2533. These compounds are structurally more compact than the chemical probe UNC1215 and maintain nanomolar L3MBTL3 potency. In addition, these compounds have profound selectivity over the Royal family proteins L3MBTL1 and MBTD1 as well as a broad range of other methyllysine readers exemplified in our AlphaScreen® assay. Through structure activity relationship studies, we deduced that a dibasic amine is necessary for compound potency as both functionalities take part in key cation–pi binding interactions with the L3MBTL3 dimer. Modifications to the (pyrrolidinyl)-piperidine showed that ligand binding is primarily mediated by the interaction of UNC2533 with the domain 2 reader pocket and that there is little room for variation in this portion of the molecule. In addition, we found that decreasing the ring size of the ethyl-pyrrolidine moiety to an ethyl-azetidine was tolerated, giving the equipotent compound 14. Most importantly, X-ray crystallography of the UNC2533-L3MBTL3 complex showed that UNC2533 binds the L3MBTL3 dimer as a 2 : 2 complex and is accommodated by rotation of the L3MBTL3 dimer interface. This is the first evidence that demonstrates the dynamic nature of the L3MBTL3 dimer and its ability to change its conformation upon ligand binding. This has implications for the design of further L3MBTL3 inhibitors and possibly histone binding.

Acknowledgements

Notes and references

1 B. D. Strahl and C. D. Allis, *Nature*, 2000, **403**, 41–45.
2 T. Jenuwein and C. D. Allis, *Science*, 2001, **293**, 1074–1080.
3 B. E. Bernstein, E. L. Humphrey, R. L. Erlich, R. Schneider, P. Bouman, J. S. Liu, T. Kouzarides and S. L. Schreiber, *Proc. Natl. Acad. Sci. U. S. A.*, 2002, **99**, 8695–8700.
4 H. Santos-Rosa, R. Schneider, A. J. Bannister, J. Sherriff, B. E. Bernstein, N. C. Emre, S. L. Schreiber, J. Mellor and T. Kouzarides, *Nature*, 2002, **419**, 407–411.
5 G. Schotta, A. Ebert, V. Krauss, A. Fischer, J. Hoffmann, S. Rea, T. Jenuwein, R. Dorn and G. Reuter, *EMBO J.*, 2002, **21**, 1121–1131.
6 D. M. Stewart, J. Li and J. Wong, *Mol. Cell. Biol.*, 2005, **25**, 2525–2538.
7 Y. B. Schwartz and V. Pirrotta, *Nat. Rev. Genet.*, 2007, **8**, 9–22.
8 Y. Zhang and D. Reinberg, *Genes Dev.*, 2001, **15**, 2343–2360.
9 G. Schotta, R. Sengupta, S. Kubicek, S. Malin, M. Kauer, E. Callen, A. Celeste, M. Pagani, S. Opravil, I. A. De La Rosa-Velazquez, A. Espejo, M. T. Bedford, A. Nussenzweig, M. Busslinger and T. Jenuwein, *Genes Dev.*, 2008, **22**, 2048–2061.
10 N. Zacharias and D. A. Dougherty, *Trends Pharmacol. Sci.*, 2002, **23**, 281–287.
11 M. Yun, J. Wu, J. L. Workman and B. Li, *Cell Res.*, 2011, **21**, 564–578.
12 S. Maurer-stroh, N. J. Dickens, L. Hughes-davies, T. Kouzarides, F. Eisenhaber and C. P. Ponting, *Trends Biochem. Sci.*, 2003, **28**, 69–74.
13 J. Kim, J. Daniel, A. Espejo, A. Lake, M. Krishna, L. Xia, Y. Zhang and M. T. Bedford, *EMBO Rep.*, 2006, **7**, 397–403.
14 F. R. Zahir, S. Langlois, K. Gall, P. Eydoux, M. A. Marra and J. M. Friedman, *Am. J. Med. Genet., Part A*, 2009, **149**, 1257–1262.
15 N. Gurvich, F. Perna, A. Farina, F. Voza, S. Menendez, J. Hurwitz and S. D. Nimer, *Proc. Natl. Acad. Sci. U. S. A.*, 2010, **107**, 22552–22557.
16 J. Qin, D. Van Buren, H. S. Huang, L. Zhong, R. Mostoslavsky, S. Akbarian and H. Hock, *J. Biol. Chem.*, 2010, **285**, 27767–27775.
17 S. V. Frye, *Nat. Chem. Biol.*, 2010, **6**, 159–161.
18 J. M. Herold, T. J. Wigle, J. L. Norris, R. Lam, V. K. Korboukh, C. Gao, L. A. Ingerman, D. B. Kireev, G. Senisterra, M. Vedadi, A. Tripathy, P. J. Brown, C. H. Arrowsmith, J. Jin, W. P. Janzen and S. V. Frye, *J. Med. Chem.*, 2011, **54**, 2504–2511.
19 J. M. Herold, L. I. James, V. K. Korboukh, C. Gao, K. E. Coil, D. J. Bua, J. L. Norris, D. Kireev, P. J. Brown, J. Jin, W. P. Janzen, O. Gozani and S. Frye, *MedChemComm*, 2012, **3**, 45–51.
20 L. I. James, D. Barsyte-Lovejoy, N. Zhong, L. Krichevsky, V. K. Korboukh, J. M. Herold, C. J. MacNevin, J. L. Norris, C. A. Sagum, W. Tempel, E. Marcon, H. Guo, C. Gao, X. P. Huang, S. Duan, A. Emili, J. F. Greenblatt, D. B. Kireev, J. Jin, W. P. Janzen, P. J. Brown, M. T. Bedford, C. H. Arrowsmith and S. V. Frye, *Nat. Chem. Biol.*, 2013, **9**, 184–191.
21 B. M. Dickson, H. Huang and C. B. Post, *J. Phys. Chem. B*, 2012, **116**, 11046–11055.
22 T. J. Wigle, J. M. Herold, G. A. Senisterra, M. Vedadi, D. B. Kireev, C. H. Arrowsmith, S. V. Frye and W. P. Janzen, *J. Biomol. Screening*, 2010, **15**, 62–71.
23 Molecular Operating Environment (MOE), 2012.10, Chemical Computing Group Inc., 1010 Sherbooke St. West, Suite #910, Montreal, QC, Canada, H3A 2R7, 2012.
24 W. Kabsch, *Acta Crystallogr., Sect. A: Found. Crystallogr.*, 1976, **32**, 922–923.
25 W. Humphrey, A. Dalke and K. Schulten, *J. Mol. Graphics*, 1996, **14**, 33–38.
26 D. Maiti, B. P. Fors, J. L. Henderson, Y. Nakamura and S. L. Buchwald, *Chem. Sci.*, 2011, **2**, 57–68.

This journal is © The Royal Society of Chemistry 2013

Med. Chem. Commun., 2013, **4**, 1501–1507 | **1507**